Determination of Distance from a 2D Picture

Institute of Physics Publishing Journal of Physics: Conference Series **52** (2006) 46–57
doi:10.1088/1742-6596/52/1/005 Mathematics for Industry in Denmark

Determination of Distance from a 2D Picture

J Gravesen[1,5], B Lassen[2], R Melnik[2,6], B Picasso[3], R Piché[4], N Radulovic[2] and L X Wang[2]

[1] Department of Mathematics, Technical University of Denmark, Matematiktorvet Building 303S, DK-2800 Kgs. Lyngby, Denmark
[2] Mads Clausen Institute, University of Southern Denmark, Grundvigs Allé 150, DK-6400 Sønderborg, Denmark
[3] Scuola Normale Superiore, Pisa, Italy
[4] Department of Mathematics, Tampere University of Technology, FIN-33101 Tampere, Finland

E-mail: J.Gravesen@mat.dtu.dk, benny@mci.sdu.dk, rmelnik@wlu.ca, radulle@mci.sdu.dk, wanglinxiang@mci.sdu.dk, b.picasso@sns.it, robert.piche@tut.fi

Abstract. An optical device is used to scan a cavity. In a single incident the scanner produces what can be considered a blurred image of the intersection curve between a plane and the cavity. Mathematically the image represents an intensity function and that is obtained by integrating a certain kernel along the intersection curve.

We suggest methods to determine the kernel and subsequently the intersection curve given the image. The methodology is tested with some success using an artificial, but realistic kernel and some synthetic images produced by this kernel.

Keywords: Optical distance measurement, inverse problem
MSC: 65K10, 68T45, 78A55

1. The problem

At the 47$^{\text{th}}$ Study Group with Industry in Gråsten, Denmark, Martin Valvik from Unisensor Inc. presented a problem concerning an optical scanner (Figure 1).

The scanner is meant to be moved inside a cavity and find its shape. The idea is first to determine a sequence of cross sections and then assemble these cross sections to give the full inner surface of the cavity. The plane which defines the cross section is fixed relative to the scanner so the position of the scanner needs to be known in order to place the cross section correctly in space. This is not the problem that concerns us here though. We only want to find the cross section relative to the scanner.

The scanner is (approximately) axisymmetric and light is transmitted in a ring round the axis down to a cone from where it is reflected radially out in a plane (approximately). If we imagine that the scanner is inserted into some cavity then the light from the scanner will hit (a part of) the sides of the cavity and form a "curve of light", the above mentioned cross section. The light will be reflected back from the sides of the cavity to the cone where it will be reflected upwards through a lens and finally make an image in the image plane.

[5] Corresponding author
[6] Present address: Wilfrid Laurier University, 75 University Avenue West, Waterloo, Ontario, N2L 3C5, Canada

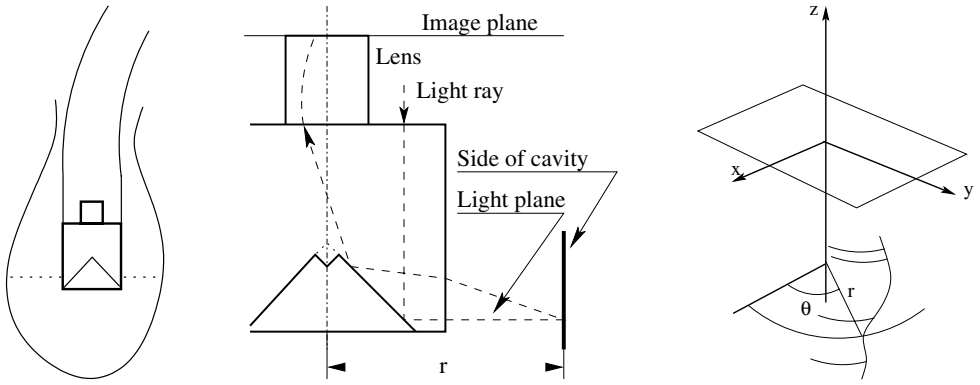

Figure 1. The scanner inside a cavity, the light path, and cylinder coordinates.

The problem is to determine the cross section from the image. So we know the intensity function $I(x, y)$ where (x, y) are coordinates in the image plane and we want to determine the function $r(\theta, z)$ where r is the distance from the axis of the scanner, θ is an angle around the center-axis (the z-axis), i.e., (r, θ, z) are cylinder coordinates.

We assume that the light is transmitted in a plane so the z dependence disappears and we are left with the task of determining the univariate function $r(\theta)$ from the intensity function $I(x, y) = I(\rho\cos\theta, \rho\sin\theta)$, where (ρ, θ) are polar coordinates in the image plane.

The paper is organized as follows. In Section 2 we explain the methodology presently used by the company and the assumptions the method is based upon and using the same assumptions we suggest an improvement to the method. in Section 3 we make a model based on more general assumptions. Mathematically we assume that the image is created by integration a certain kernel along the intersection curve. In Section 4 we explain how the kernel can be determined experimentally. We note that the problem at hand is related to shape-from-shading problems and we explore this connection further in Section 5. In this section we also explain how, by using the kernel mentioned above, we can obtain the intersection curve from an image by solving an optimization problem. In Section 6 we give an example of this procedure and the results are presented in Section 8. We did not have enough data to determine the kernel so instead we postulated a kernel we deemed reasonable. In Section 7 we use the singular value decomposition to check how well the postulated kernel could explain the image created by a point source. Finally in Section 9 we have the conclusions.

The people working on the problem was: Ole Brink-Kjær, Kasper Doring, Jens Graven, Jens Karlsson, Poul G. Hjorth, Benny Lassen, Roderick Melnik, Henrik Gordon Petersen, Bruno Picasso, Robert Piche, Janis Rimshans, Nenad Radulovic, Peter Røgen, Martin Valvik, Linxiang Wang, Stefan Wolff.

We will like take this opportunity to thank Unisensor and in particular Martin Valvik for contributing the problem, answering many questions during the study group, and even organizing new measurements when requested.

2. The present method and an improvement

The methodology presently used by the company builds upon a number of assumptions.

(i) It is assumed that the light from the scanner is reflected in a plane orthogonal to the axis so the only part of the cavity that can be "seen" is the intersection of the cavity with this plane, i.e, we only need to determine a function of one variable $r(\theta)$.

(ii) More severely, it is assumed that the image intensity along a radial ray, i.e., $I(x, y) = I(\rho\cos\theta, \rho\sin\theta)$ depends only on the distance $r = r(\theta)$ in this direction.

The point of view is that the point $\rho_{\max}$ where the function $I(\rho) = I(\rho\cos\theta, \rho\sin\theta)$ has its maximum is *the* image of the point $r(\theta)$, and that there is a one-to-one correspondence between r and $\rho_{\max}$. The function $\rho_{\max} \mapsto r$ can subsequently be determined experimentally. The scanner will never be exactly axisymmetric but that only means that $\rho_{\max}$ also depends on θ, i.e., we need to experimentally determine the function $(\theta, \rho_{\max}) \mapsto r$.

Given the assumptions 1) and 2) above, the basic problem is to determine the maximum intensity $I(\rho) = I(\rho\cos\theta, \rho\sin\theta)$ along a radial ray. First of all it is necessary to smooth the function before the maximum is determined, cf. Figure 4 where the lefthand graph shows the intensity along a radial ray. Furthermore the intensity function is often flat and hence it can be difficult and error prone to determine the maximum.

Instead of considering the maximum as the image of the point $r(\theta)$ it is better to consider the whole function $I(\rho) = I(\rho\cos\theta, \rho\sin\theta)$ as the result of a measurement and then use a more robust and easily calculated number to characterize the function. An obvious choice is to use the first moment (center of mass):

$$\rho_0 = \frac{\int_0^\infty \rho I(\rho)\,\mathrm{d}\rho}{\int_0^\infty I(\rho)\,\mathrm{d}\rho}, \tag{1}$$

as ρ_0 is insensitive to noise there is no need to perform any smoothing. The two functions $r(\rho_0)$ and $r(\rho_{\max})$ are both decreasing and exhibit the same qualitative behaviour. It is of course possible to incorporate asymmetry in this setting too, and determine the function $r(\theta, \rho_0)$ experimentally.

3. The basic model

We consider a cavity given by the equation $r = r(\theta, z)$ and assume that the light from the scanner is reflected diffusively with intensity $\alpha(r, z)$ from the point with cylinder coordinates $(r(\theta, z), \theta, z)$. If $(x, y) \mapsto G_0(x, y, r, \theta, z)$ is the intensity function created by a (unit) light source situated at the point (r, θ, z), then the intensity in the image plane created by the intensity function $\alpha(r, z)$ is found by integrating $G(x, y, r, \theta, z) = \alpha(r, z)G_0(x, y, r, \theta, z)$ over the surface of the cavity.

$$I(x, y) = \int_0^{2\pi} \int_{-\infty}^{\infty} G(x, y, r(\theta, z), \theta, z)\,\mathrm{d}z\,\mathrm{d}\theta. \tag{2}$$

A small remark is appropriate here. The intensity α at a point on the surface depends not only on the distance but also on the angle between the light ray and the normal of the surface. Also, the integration should be with respect to surface area and not $\mathrm{d}z\,\mathrm{d}\theta$. What happens is that light transmitted in small angle $\Delta\theta\Delta z$ can be distributed on a larger area of the surface and thus the intensity falls, but when we then integrate with respect to surface area we regain all the intensity, so the two corrections cancels each other, and (2) is correct.

In practice there would only be a small z-interval where $G(x, y, r(\theta, z), \theta, z) \neq 0$. If we can assume that the light from the scanner only emits light in a plane orthogonal to the symmetry axis, then we can drop the z dependence and we have diffuse light emitted from a curve with equation $r = r(\theta)$ and we have a kernel $G(x, y, r, \theta) = \alpha(r)G_0(x, y, r, \theta)$, where $\alpha(r) = 1/r$. The intensity is now

$$I(x, y) = \int_0^{2\pi} G(x, y, r(\theta), \theta)\,\mathrm{d}\theta, \tag{3}$$

and we want to determine the function $r(\theta)$. There are now two tasks

(i) Determine the kernel $G(x, y, r, \theta)$.

(ii) Provide a procedure that determines the function $r(\theta)$ from the intensity $I(x, y)$.

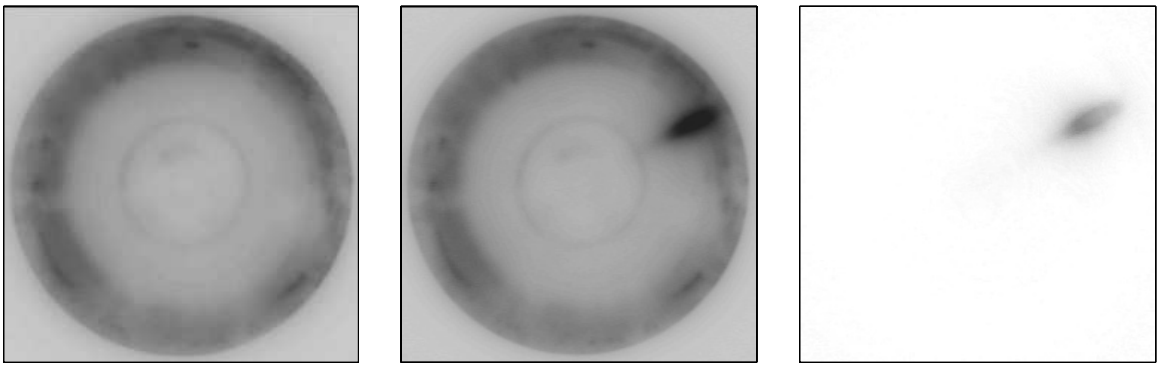

Figure 2. Inverted images: the reference, the thin stick, and the difference.

4. The kernel

If we assume that the scanner is symmetric then we have

$$G(x, y, r, \theta) = G(x\cos\theta - y\sin\theta, x\sin\theta + y\cos\theta, r, 0) \tag{4}$$

so we need only to determine $G(x, y, r, 0)$.

It is tempting to try to calculate the kernel from first principles. It is indeed possible to use geometric optics and follow a ray from a point in the "light"-plane through the scanner until it hits the image plane. This gives a map from a sphere centered at the light source to the image plane and the area deformation gives (a part of) the intensity, i.e., the kernel. The actually computations are rather involved and it will be hard (but not impossible) to get a usable result.

Unfortunately there is a more severe and fundamental problem. When the ray hits a boundary between two media, eg. at the cone or at the outside of scanner, a fraction of the light is transmitted and the other fraction gets reflected. These fractions depends not only on the angle between the ray and the surface normal, but also on the *polarization* of the light, cf. [7]. That in turn depends on the light source, the material of the cavity, and optical details of the scanner and would in practice be impossible to determine.

Instead we suggest to determine the kernel experimentally. The method would be to use the scanner, not to make a "picture" of a cavity, but to make a series of pictures of a thin stick in known distances r_k from the axis of the scanner. If the stick is sufficiently thin, then we can subtract a reference picture (a picture of nothing) and get a direct measurement of the kernel $G(x_i, y_j, r_k, 0)$. where (x_i, y_j) are the coordinates of the pixels of the CCD-camera, see Figure 2. Sufficiently thin would mean thinner than the final resolution that the scanner is supposed to provide.

After obtaining the values $G(x_i, y_j, r_k, 0)$ the next step is to approximate the kernel function with a suitable smooth function, for example a trivariate tensor product B-spline.

For a fixed r we can see from Figure 2 that the support of the kernel is concentrated in a relatively small area. Hence we concentrate the knots in that same area, cf. Figure 3. When we now let r vary two things happens. The shape of the intensity function changes, and the position of the support is shifted along the x-axis. We have two suggestions to model the kernel. The first is as a straight forward B-spline, cf. [3]

$$G(x, y, r, 0) \approx f(x, y, r) = \sum_{i,j,k} f^{i,j,k} N_i^{n_1}(x, \mathbf{x}) N_j^{n_2}(y, \mathbf{y}) N_k^{n_3}(r, \mathbf{r}), \tag{5}$$

where $N_i^n(t, \mathbf{t})$ denotes the i^{th} basis function of degree n on the knot vector $\mathbf{t}$ and the knots $\mathbf{x}$ in the x-direction is chosen such that they can accommodate all positions of the support. The

coefficients $f^{i,j,k}$ are chosen such that they minimize the 2-norm:

$$\sum_{i,j,k} \left(f(x_i, y_j, r_k) - G(x_i, y_j, r_k, 0)\right)^2. \tag{6}$$

This is a linear problem which is easily solved. For the second suggestion we shift the origin to the first moment (the center of mass) of the intensity function, and propose an approximation to the kernel of the following form:

$$G(x, y, r, 0) \approx f(x - x_0(r), y, r) \tag{7}$$

where x_0 and f are B-splines

$$x_0(r) = \sum_i x_0^i N_i^{n_0}(r, \mathbf{r}_0), \tag{8}$$

$$f(x, y, r) = \sum_{i,j,k} f^{i,j,k} N_i^{n_1}(x, \mathbf{x}) N_j^{n_2}(y, \mathbf{y}) N_k^{n_3}(r, \mathbf{r}). \tag{9}$$

The coefficients x_0^i and $f^{i,j,k}$ are chosen such that they minimize the 2-norm:

$$\sum_k \left(x_0(r_k) - \frac{\sum_{i,j} x_i G(x_i, y_j, r_k, 0)}{\sum_{i,j} G(x_i, y_j, r_k, 0)} \right)^2 \tag{10}$$

and

$$\sum_{i,j,k} \left(f(x_i - x_0(r_k), y_j, r_k) - G(x_i, y_j, r_k, 0)\right)^2 \tag{11}$$

This leads to two linear problems which are easily solved. It will in both cases be necessary to experiment with the degrees $(n_0,)$ n_1, n_2, n_3 and the number and placements of the knots $(\mathbf{r}_0,)$ $\mathbf{x}, \mathbf{y}, \mathbf{r}$. The first suggestion needs more coefficients, but the structure is simpler so subsequent calculations are easier.

There is potentially another advantage of the form (5). Suppose the r-dependents of the kernel is so simple that it can be approximated by a low degree polynomial, of degree K. Then it is possible to pre-compute some values we will later need in a minimization procedure where we try to find the function $r(\theta)$ that makes $\int G(x_i, y_j, r(\theta), \theta)\,\mathrm{d}\theta$ fits the measurement best. Indeed, if $r(\theta)$ is a uniform B-spline, $r(\theta) = \sum_\ell a_l N_\ell^m(\theta - 2\pi\ell/n)$, then

$$\begin{aligned} &G(x_i, y_j, r(\theta), \theta) = f(x_i \cos\theta - y_j \sin\theta, x_i \sin\theta + y_j \cos\theta, r(\theta)) \\ &= \sum_{i,j,k} f^{i,j,k} N_i^{n_1}(x_i \cos\theta - y_j \sin\theta) N_j^{n_2}(x_i \sin\theta + y_j \cos\theta) \left(\sum_\ell a_\ell N_\ell^m \left(\theta - \frac{2\pi\ell}{n} \right) \right)^k. \end{aligned}$$

For $\theta \in [2\pi\ell/n, 2\pi(\ell+1)/n]$ only $m+1$ of the basis functions $N_\ell^m\left(\theta - \frac{2\pi\ell}{n}\right)$ are non-zero so we have

$$\int_0^{2\pi} G(x_i, y_j, r(\theta), \theta)\,\mathrm{d}\theta = \sum_{k=1}^{K} \sum_{\ell_1, \ldots, \ell_k} G_{i,j}^{\ell_1, \ell_2, \ldots, \ell_k} a_{\ell_1} a_{\ell_2} \ldots a_{\ell_k}, \tag{12}$$

where the inner sum is over sequences $\ell_1 \le \ell_2 \le \ldots \le \ell_k$ with $l_k - l_1 \le m$ and where the coefficients $G_{i,j}^{\ell_1, \ell_1, \ldots, \ell_k}$ can be precomputed. If the degrees m and K are sufficiently small then the number of coefficients $G_{i,j}^{\ell_1, \ell_1, \ldots, \ell_k}$ is manageable.

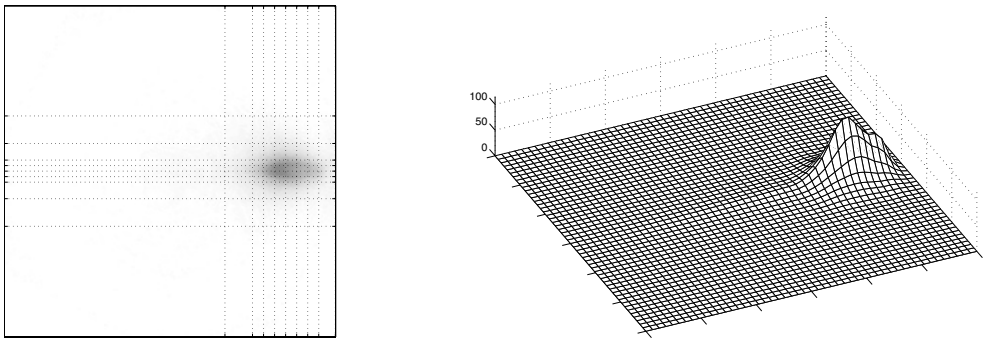

Figure 3. To the left the rotated image with the knots lines, to the right the quadratic B-spline approximating the intensity.

As a small test we have rotated the image in Figure 2, with 600×600 pixels, and values between 0 and 117. We have used a quadratic tensor product B-spline to approximate the intensity function, and the knot-vectors were

$$\mathbf{x} = 0, 400, 450, 470, 490, 510, 530, 550, 570, 600,$$
$$\mathbf{y} = 0, 200, 250, 280, 290, 300, 310, 320, 350, 400, 600.$$

The result can be seen in Figure 3. The approximation error measured in the max-norm, the 2-norm, and the 1-norm became

$$\|I - f\|_\infty = 15.6, \qquad \|I - f\|_2 = 1.27, \qquad \|I - f\|_1 = 0.50.$$

5. The procedure

We now have our approximation of the kernel $G(x, y, r, \theta)$, i.e., we assume that

$$G(x, y, r, \theta) = f(x\cos\theta - y\sin\theta, x\sin\theta + y\cos\theta, r), \qquad \text{or} \tag{13}$$
$$G(x, y, r, \theta) = f((x - x_0(r))\cos\theta - y\sin\theta, (x - x_0(r))\sin\theta + y\cos\theta, r). \tag{14}$$

Given measured intensities $I(x_i, y_j)$, we want to determine a function $r(\theta)$ such that (3) is satisfied. This is a non-trivial problem which is closely related to the so-called shape-from-shading problems. In what follows we highlight briefly this connection. Recall that our original problem described in Section 1 requires determining the shape of an object (a cavity in our case) from its two-dimensional images. In its essence, this is a special case of the classical shape-from-shading problem that has been discussed extensively in the literature [4, 10, 12, 9, 6, 13]. Basic steps upon which the model construction for this problem and the procedure for its solution can be based are as follows. As before, we will denote by $I(x, y)$ the intensity function of the image. In order to determine the shape (a surface) of the object on the basis of the given image(s), one could relate the intensity (or the brightness) function of the image (given, for example, at each pixel (x_i, y_j)) and the reflectance map that keeps the information on the real three-dimensional object. The form of the reflectance map, under which the images are generated from the (unknown) 3D depth map, has to be assumed as the only measurements produced by the scanner that can be analysed are the images themselves [13]. A natural way to relate such images to the 3D object is via the surface depth (the distance or the hight) function in

the z-direction, denoted further by $u(x, y)$. Then, images of the same object, given in the (x,y)-plane, will differ from each other by shape gradients $\zeta_1 = \partial u/\partial x$ and $\zeta_2 = \partial u/\partial y$ which are essential characteristics of the 3D object. Hence, one can view the information based on the set of functions $u(x, y)$, ζ_1, and ζ_2 as the information from which, among other things, the shape of cavity can be extracted. As the cavity shape is modelled in (2) by using function $r(\theta, z)$ that enters the kernel of the integral equation, the development of specific algorithms to obtain r from (u, ζ_1, ζ_2) would be dependent on the specific form of kernel approximation in model (2). In order to determine u (and hence ζ_1 and ζ_2) recall that "shading", a 2D characteristic of the object, is represented mathematically by the image intensity $I(x, y)$, while "shape", a 3D characteristic of the object, is represented by the surface reflectance denoted here by $H(\zeta_1, \zeta_2)$. The latter specifies the reflectance of a surface under consideration as a function of its orientation and both functions are related to each other by the image irradiance equation (e.g., [4])

$$I(x, y) = H(\zeta_1(x, y), \zeta_2(x, y)), \quad \zeta_1 = \partial u/\partial x, \quad \zeta_2 = \partial u/\partial y. \tag{15}$$

Problem (15) can be reformulated as the first order partial differential equation under appropriate assumptions on function H. According to the Unisensor representative, the assumption of perfectly matt (Lambertian) surface is reasonable, hence we can use Lambert's law to determine a possible approximation to H. In particular, if a part of the surface with normal vector $\mathbf{n} = (-u_x, -u_y, 1)$ is illuminated in the direction $\mathbf{l} = (l_1, l_2, l_3)$, the emitted radiance (that will determine the image produced by the scanner) is given by the cosine of the angle between $\mathbf{n}$ and $\mathbf{l}$, namely by $(l_3 - l_1 u_x - l_2 u_y)/(u_x^2 + u_y^2 + 1)^{1/2}$. Therefore, if, for example, $\mathbf{l} = (0, 0, 1)$, then under the assumption of unit albedo and unit power of the source light, we arrive at the Hamilton-Jacobi equation of the form (e.g., [9]):

$$(u_x^2 + u_y^2 + 1)^{-1/2} = I(x, y). \tag{16}$$

In a more general situation, $\mathbf{l} = (\sin\sigma_l \cos\tau_l, \sin\sigma_l \sin\tau_l, \cos\sigma_l)$, where σ_l and τ_l are slant and tilt angles [2]. The latter expression can be simplified if we consider cross-sectional areas only, as depicted in Fig. 2, to $\mathbf{l} = (\cos\tau_l, \sin\tau_l, 0)$. Then, accounting for the surface albedo (denoted by λ) and the incident light flux (denoted by ρ), we obtained the following approximation to function $H(\zeta_1, \zeta_2)$:

$$H(\zeta_1, \zeta_2) = \lambda\rho \frac{-\zeta_1 \cos\tau_l - \zeta_2 \sin\tau_l}{\sqrt{1 + \zeta_1^2 + \zeta_2^2}}. \tag{17}$$

Given (15) and (17) we obtain the first order PDE with respect to the distance (or surface depth) function $u(x, y)$. According to the Unisensor representative, all parameters in this equation are measurable, including grayness of the surface λ, the incident light flux ρ (a characteristic of the scanner), while σ_l and τ_l can be estimated on the basis of the image intensity map (given by the company), physical characteristics of the surface and the scanner (e.g., [12, 13] and references therein). A natural way to solve the resulting problem is by applying the variational approach (e.g., [4, 8]). In this case, the cost functional can be defined as follows:

$$W = \iint_\Omega \left\{ [I - H]^2 + \mu_1 \left[\left(\frac{\partial^2 u}{\partial x^2} \right)^2 + 2 \left(\frac{\partial^2 u}{\partial x \partial y} \right)^2 + \left(\frac{\partial^2 u}{\partial y^2} \right)^2 \right] + \mu_2 \Phi \right\} \mathrm{d}x\, \mathrm{d}y \to \min, \tag{18}$$

where the second term (known as the "departure-from-smoothness" error) is a regularizing term, as the problem at hand is an ill-posed problem (see, [4, 12, 5]). The first term (known as the "ring of light" or "brightness" error) comes into consideration directly from equation (15), while the third term is added to ensure integrability of the constrained optimization problem.

Models (2) and (17) are related in a sense that both are attempts to construct a model that relates the information about a 3D object and the information about 2D images of that object.

While in the former case, we use a geometric analysis of the problem to construct the model, the latter approach is ultimately based on a more conventional idea of using energy functionals (e.g., [1]). In our case, instead of using a more conventional approximation (17), we attempt to approximate the kernel of the reflectance map as it is stated by our formula (2). In this case, we model $r(\theta)$ (rather than function $u(x, y)$) as a uniform periodic B-spline

$$r(\theta) = \sum_{k=1}^{n} a_k N^m \left(\frac{n}{2\pi}\theta - k \right), \tag{19}$$

where N is the B-spline of degree m on the uniform knot sequence $\ldots, -1, 0, 1, \ldots$ and n is sufficiently large to give the resolution we want. The coefficients a_k are chosen such that the 2-norm

$$\sum_{i,j} \left(I(x_i, y_j) - \int_0^{2\pi} G(x_i, y_j, r(\theta), \theta)\, \mathrm{d}\theta \right)^2$$

is minimized. As the integral in (18) is replaced by a finite sum, the third term (18) is not needed. Furthermore, since the problem will be solved in terms of coefficients a_k which will determine $r(\theta)$ by (19), we use the quadratic term $\|a_k\|^2$ to regularize the problem. In its essence, our approach has some similarities with the Green's function approach to shape-from-shading (e.g., [11]). Now, the task at hand is the following optimisation problem:

$$\text{minimize } \sum_{i,j} \left(I(x_i, y_j) - \int_0^{2\pi} G(x_i, y_j, r(\theta), \theta)\, \mathrm{d}\theta \right)^2 + \mu \|a_k\|^2, \tag{20}$$

where μ is a parameter and $\|\cdot\|$ is a suitable seminorm, common choices include

$$\|a_k\|^2 = \sum_k a_k^2, \quad \|a_k\|^2 = \sum_k (a_k - a_{k-1})^2, \quad \|a_k\|^2 = \sum_k (a_k - 2a_{k-1} + a_{k-2})^2.$$

An important aspect of this type of problems is to obtain a good initial guess for $r(\theta)$. The scanner will be moved slowly inside the cavity so we would have a series of images, i.e., intensity functions, from which we want to determine planar sections of the cavity, i.e., $r(\theta)$. We expect the planar section of two subsequent measurements to be very similar, so the result of the optimization of one measurement, would be a very good initial guess for the next. To bootstrap this procedure and have a good guess for the very first image one could use prior knowledge of the cavity or the simplified procedure suggested in section 2.

In Section 6 we give an example of this procedure. We did not have sufficient data to make a reasonable B-spline model of the kernel so instead we postulate a kernel with an exponential decay and a $1/r$ dependence.

We conclude this section with the following remark. The problem at hand is a strongly non-linear problem and it would be advantageous to reduce it (at least for some special cases) to a sequence of linear problems. For model (17) it can be done if we use the assumption that the real shape of the object is smooth. Then, the equation $I(x, y) = H(\zeta_1, \zeta_2)$ can be approximated by using Taylor's expansion of the reflectance function (e.g., [10]). As a result, it is easy to find the Fourier transforms F_{ζ_1} and F_{ζ_2} in terms of the Fourier transform of of $u(x, y)$. This allows to relate the Fourier spectrum of the image and the Fourier transform of the surface. Finding Fourier's inverse of F_u will allow to estimate the object shape. This simplification should be useful when the Unisensor needs to analyse sufficiently smooth surfaces without substantial irregularities.

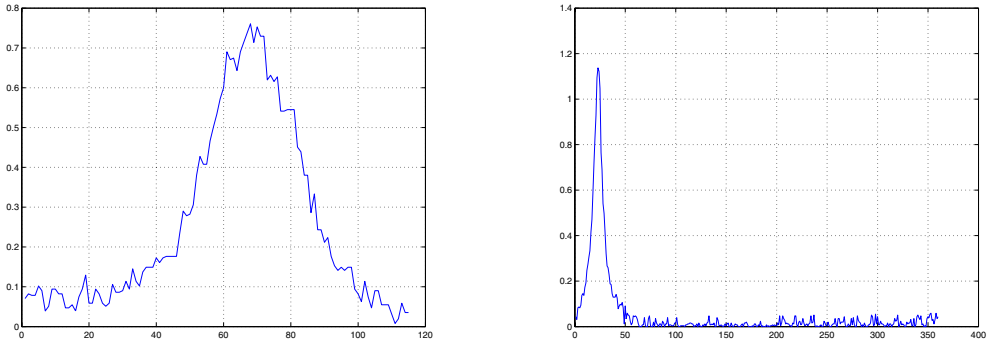

Figure 4. To the left the radial part $f(\rho)$ and to the right the angular part $g(\alpha)$ of intensity distribution $I(\rho, \alpha)$.

6. Case study example

For the case study we make some changes to the situation in Section 5. Instead of Cartesian coordinates (x, y) in the image plane we use polar coordinates (ρ, α), and instead of using B-splines to describe the kernel, we just postulate a kernel of the form

$$G(\rho, \alpha, r, \theta) = Ae^{-k_1(\rho - k_3/r)^2 - k_2(\alpha-\theta)^2} = Ae^{-k_1(\rho-k_3/r)^2} e^{-k_2(\alpha-\theta)^2}, \tag{21}$$

i.e., the product of two Gaussian. The parameters A, k_1, and k_2 are chosen such that the Gaussian approximates the the functions $f(\rho)$ and $g(\alpha)$ from Figure 4. The result was $A = 345$, $k_1 = 0.002$, and $k_2 = 0.01$. We had only data for three unknown values of r so we had no ways of estimating k_3 and we just put $k_3 = 1$. This gives us a predicted intensity as follows:

$$H = \int_0^{2\pi} 345e^{-0.002(\rho - 1/r(\theta))^2 - 0.01(\alpha-\theta)^2} \, \mathrm{d}\theta. \tag{22}$$

The function r is represented by a vector $r = (r_1, r_2, ..., r_n)$, (can be thought as a discretisation in θ), and as regularization term we chose $\|r\|^2 = \frac{2\pi}{n} \sum_{i=1}^{n} (r_i)^2$. So the functional to minimise has the following form

$$\int_{\rho=0}^{\infty} \int_{\alpha=0}^{2\pi} \left\{ [I - H]^2 + \mu \|r\|^2 \right\} \, \mathrm{d}\alpha \, \mathrm{d}\rho \to \min . \tag{23}$$

where $I(\alpha, \rho)$ is the measured image intensity.

At this stage we took $r = 1$, corresponding to a unit circular object, and created a synthetic image using (22). We then tested the optimization procedure by letting the initial guess of r be randomly chosen around $r = 1$ with a relative error of 5%. The maximal initial relative error we have tried is 20%. Numerical experiments show that the optimization gives a quite good estimation of the actual value of r, as shown in figure 6 to 8.

7. Considerations regarding the Singular Values Decomposition

In this section we provide details of our SVD-based procedure to verify how well the kernel postulated in Section 6 can explain the image created by a point source. We have discretized ρ and α:

$$\begin{aligned} \rho &= \rho_i \qquad & i &= 1, \ldots, N, \\ \alpha &= \alpha_j \qquad & j &= 1, \ldots, M . \end{aligned}$$

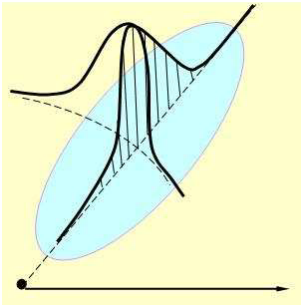

Figure 5. The assumption that $\mathrm{I}(\rho,\alpha)$ factors as is given by (24).

The intensity distribution $I(x,y)$ obtained processing the CCD picture generated by a source in position (r,θ) has been transformed into a discrete polar–coordinate function $\tilde{I}(\rho_i,\alpha_j)$: we denote by $\tilde{I}\in\mathbb{R}^{N\times M}$ the matrix $\tilde{I}_{i,j}\equiv\tilde{I}(\rho_i,\alpha_j)$.

The assumption (see Fig.5) that $I(\rho,\alpha)$ factors as

$$I(\rho,\alpha)=f(\rho)\cdot g(\alpha) \tag{24}$$

corresponds to the fact that the matrix $\tilde{I}$ has rank 1. Of course the numerical matrix $\tilde{I}$ has full rank, anyway we can get a measure of "how far" is that matrix from having rank 1 by analysing the singular values decomposition (SVD) of $\tilde{I}$. In fact:

$$\tilde{I}=USV^t \quad \text{with} \quad U\in\mathbb{R}^{N\times N},\quad S\in\mathbb{R}^{N\times M},\quad V\in\mathbb{R}^{M\times M},$$

where U and V are unitary matrices and $S=\mathrm{diag}(\sigma_i)$, $i=1,\dots,\min\{N,M\}$. The numbers $\sigma_1\geq\sigma_2\geq\cdots\geq 0$ are the singular values of $\tilde{I}$. Denote by u_i and v_i the i^{th} column of the matrices U and V respectively. If $\sigma_2\ll\sigma_1$ then $\tilde{I}$ is well approximated by the matrix $\tilde{I}_1=\sigma_1\cdot u_1v_1^t$ which has rank 1: it holds that $\|\tilde{I}-\tilde{I}_1\|_2\leq\sigma_2$. In this case $\sigma_1\cdot u_1$ and v_1 can be taken as a discrete version of $f(\rho)$ and $g(\alpha)$ respectively.

Indeed our calculations showed that there were at least 10 singular values not negligible: in that case the matrix is well approximated by $\tilde{I}_{10}=\sum_{i=k}^{10}\sigma_ku_kv_k^t$ that has rank 10 and is such that $\|\tilde{I}-\tilde{I}_{10}\|_2\leq\sigma_{11}$. If it is possible to find ten pairs of simple functions (f_k,g_k) such that $\sigma_ku_k\approx f_k(\rho_i)$ and $v_k\approx g_k(\alpha_i)$ then $\sum_k f_k(\rho)g_k(\alpha)$ is a good approximation to the kernel. This has not been investigated in further detail. Note also that for this procedure to be useful in practice, the r-dependence of the kernel should be simple.

8. Results of computations

To find optimal values for μ and n in (23) we chose to fix μ and then carry out calculations for $n=20,40$ and 80. We did calculations for $\mu=10^{-6},10^{-3},0.05$ and 0.1. In order to estimate the error in the minimized function we used the $\mathcal{L}^2$ norm on the difference between the exact function ($Z=1$) and the minimized function. Those numbers are shown in Table 1 together with the time it took to carry out the minimizations. The best value we found was $\mu=0.05$ and the more discretisation points the better. In Figure 6 to 8 the initial guess and the minimized function are shown for different values of μ.

The target function is extremely simple (a constant), as is the kernel, so it is not possible to draw any hard conclusions regarding the usuability of the procedure. That will require more realistic data and extensive testing.

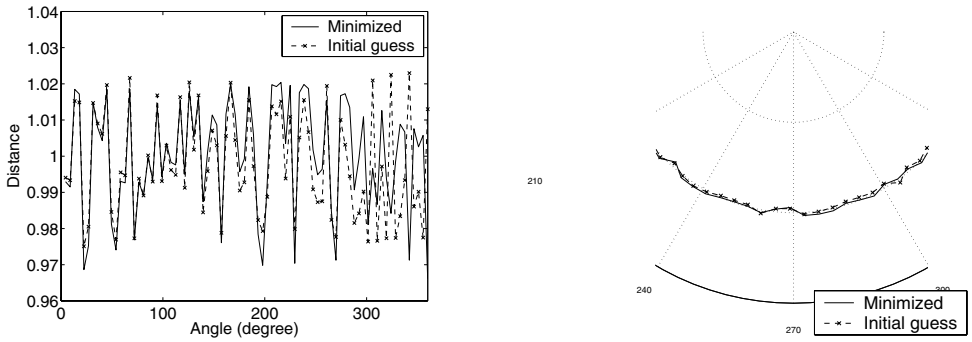

Figure 6. To the left a plot of the initial guess and the minimized distance function as a function of angle, to the right a section of a plot the initial guess and minimized function, for $\mu = 10^{-6}$ and $n = 80$.

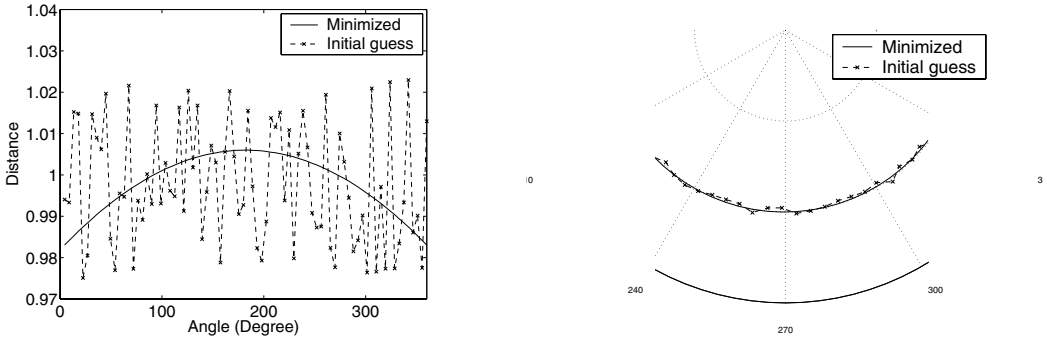

Figure 7. To the left a plot of the initial guess and the minimized distance function as a function of angle, to the right a section of a plot the initial guess and minimized function, for $\mu = 0.05$ and $n = 80$.

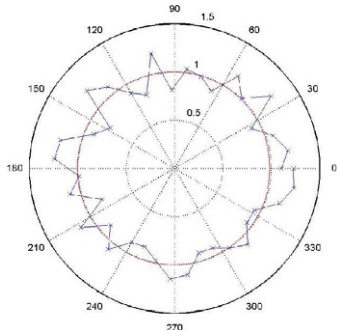

Figure 8. A plot of the the initial guess and minimized function for $\mu = 0.05$ and $n = 80$. The initial guess was generated with 20% random noise

9. Discussion and conclusion

We have demonstrated that the image produced by the scanner can be calculated by integrating a kernel along the "curve of light", cf. (3). The kernel can for a fixed r be represented well by a tensor product B-spline of a reasonable size, cf. (5) or (7).

$\mu \setminus n$	20		40		80	
10^{-1}	0.22%	17 sec	0.16%	61 sec	0.11%	464 sec
0.05	0.17%	12 sec	0.12%	52 sec	0.08%	90 sec
10^{-3}	0.29%	6 sec	0.15%	36 sec	0.09%	179 sec
10^{-6}	0.3%	5 sec	0.27%	6 sec	0.17%	80 sec

Table 1. The relative error and timing for different values of n and μ.

As an other approach, the singular value decomposition suggest that it is possible to describe the kernel as the sum of the products of ten pairs of univariate functions, cf. Section 7. So it might be possible to use something more simple than the tensor product B-spline descriptions, the univariate functions above would have to be described by a few parameters. But we have not investigated that.

We did not have enough data to model the r dependence of the kernel so there is a need for more work here, first of all images of "point sources" in known distances are needed.

Using a variational approach we have shown that it is possible to recapture the "curve of light" from the image. As the r dependence was unknown we used an artificial but realistic kernel, and we expect to get similar results using a more correct kernel. Once more it is necessary to do extensive testing with real data.

The timings given in Section 8 are not encouraging, but improvements can be made. The function $r(\theta)$ depends linearly on the coefficients a_k so it is not hard to get the gradient and Hessian of the objective function given in (20), all it takes is to differentiate (13) or (14) with respect to r, i.e., we only have to differentiate a number of B-splines. Access to the gradient and Hessian will speed the optimization up substantially, as will an implementation in C or Fortran. Also it is perhaps possible to pre-compute a substantial part of the objective function, cf. (12). Finally, since we deal with an inverse problem, some prior knowledge of the cavity should help improve the performance of the methodologies developed and tested in this contribution.

References

[1] Chan, T.F., Variational PDE models in image processing, *Notices of the AMS*, **50(1)**, 2003, 14–26.

[2] Chojnacki, W., Brooks, M.J., Gibbins, D., Revisiting Pentland's estimator of light source direction, *J. Opt. Soc. Am. A*, **11**, 1994, 118–124.

[3] de Boor, C., *A Practical Guide to Splines*, Springer-Verlag, New York 2001.

[4] Horn, B.K.P. and Brooks, M.J., *Shape from Shading*, MIT Press, Cambridge, MA, 1989.

[5] Hsieh, J.-W. et al Wavelet-based shape from shading, *Graphical Models and Image Processing*, **57(4)**, 1995, 343–362.

[6] Jones, A.G. and Taylor, C.J., Robust shape from shading, *Image and Vision Computing*, **12(7)**, 1994, 411–421.

[7] Landau, L.D. and Lifshitz, E.M., *Electrodynamics of Continuous Media*, Course of Theoretical Physics Vol. 8, Pergamon Press, Oxford 1960.

[8] Lepsky, O., Hu, C., and Shu, C-W., Analysis of the discontinuous Galerkin method for Hamilton-Jacobi equations, *Appl. Numerical Mathematics*, **33**, 2000, 423–434.

[9] Lions, P.L., Rouy, E., and Tourin, A., Shape-from-Shading, viscosity solutions and edges, *Numerische Mathematik*, **64(3)**, 1993, 323–353.

[10] Pentland, A.P., Linear shape from shading, *Int. J. of Computer Vision*, **4**, 1990, 153–162.

[11] Torreao, J. R. A., A Green's function approach to shape from shading, *Pattern Recognition*, **34**, 2001, 2367–2382.

[12] Zheng, Q. and Chellappa, R., Estimation of illuminant direction, albedo, and shape from shading, *IEEE Trans. on Pattern Analysis and Machine Intelligence*, **13(7)**, 1991, 680–702.

[13] Zhao, W. and Chellappa, R., Symmetric shape-from-shading using self-ratio image, *Int. J. of Computer Vision*, **45(1)**, 2001, 55–75.